Received: 5 September 2022 | Revised: 17 December 2022 | Accepted: 3 May 2023

DOI: 10.1002/jbm.b.35268

RESEARCH ARTICLE

Society For Biomaterials | WILEY

In vitro biocompatibility of polylactide and polybutylene succinate blends for urethral tissue engineering

Reetta Sartoneva[1,2,3] | Inari Lyyra[1] | Maiju Juusela[1] | Vipul Sharma[1] | Heini Huhtala[4] | Jonathan Massera[1] | Minna Kellomäki[1] | Susanna Miettinen[1,3]

[1]Faculty of Medicine and Health Technology (MET), Tampere University, Tampere, Finland

[2]Department of Obstetrics and Gynaecology, The Hospital District of South Ostrobothnia, Seinäjoki, Finland

[3]Tays Research Services, Wellbeing Services County of Pirkanmaa, Tampere University Hospital, Tampere, Finland

[4]Faculty of Social Sciences, Tampere University, Tampere, Finland

Correspondence
Reetta Sartoneva, Tampere University, Arvo Ylpön katu 34, 4th floor 33520 Tampere, Finland.
Email: reetta.sartoneva@tuni.fi

Funding information
Academy of Finland, Grant/Award Numbers: 339405/RS, 312413/SM; Competitive Research Funding of the Pirkanmaa Hospital District, Grant/Award Number: 9AB069; Finnish Medical Foundation, Grant/Award Number: 3856; TAU Graduate School; Tekniikan Edistämissäätiö

Abstract

Surgical treatment of urothelial defects with autologous genital or extragenital tissue grafts is susceptible to complications. Tissue engineering utilizing novel biomaterials and cells such as human urothelial cells (hUC) for epithelial regeneration and adipose stromal cells (hASC) for smooth muscle restoration might offer new treatment options for urothelial defects. Previously, polylactide (PLA) has been studied for urethral tissue engineering, however, as such, it is too stiff and rigid for the application. Blending it with ductile polybutylene succinate (PBSu) could provide suitable mechanical properties for the application. Our aim was to study the morphology, viability and proliferation of hUC and hASC when cultured on 100/0 PLA/PBSu, 75/25 PLA/PBSu blend, 50/50 PLA/PBSu blend, and 0/100 PLA/PBSu discs. The results showed that the hUCs were viable and proliferated on all the studied materials. The hUCs stained pancytokeratin at 7 and 14 days, suggesting maintenance of the urothelial phenotype. The hASCs retained their viability and morphology and proliferated on all the other discs, except on PLA. On the PLA, the hASCs formed large aggregates with each other rather than attached to the material. The early smooth muscle cell markers SM22α and α-SMA were stained in hASC at 7 and 14 day time points on all PBSu-containing materials, indicating that hASCs maintain their smooth muscle differentiation potential also on PBSu. As a conclusion, PBSu is a highly potential biomaterial for urothelial tissue engineering since it supports growth and phenotypic maintenance of hUC and smooth muscle differentiation of hASC.

KEYWORDS
adipose stromal cells (ASC), polybutylene succinate (PBSu), polylactide (PLA), polymer blends, urethral tissue engineering, urothelial cells (UC)

1 | INTRODUCTION

Urethral defects are common due to various reasons, such as traumas, strictures, or congenital malformations. Yet the surgical reconstruction of these defects is challenging. Smaller defects are mainly treated with urethroplasty using genital tissue graft or flaps. However, in more severe defects, non-genital tissue grafts, such as bladder acellular matrix or buccal mucosa, are used. The extragenital

non-cellular tissue grafts are not optimal for urethral reconstruction. Complications, such as fistulas, strictures, shrinkage, or residual curvature, are common.[1–3] Therefore, there is a need for developing new graft materials and techniques for severe urethral defect reconstructions.

Tissue engineering could provide solutions for urethral reconstruction, aiming to overcome problems related to the traditional surgical techniques. The selection of optimal biomaterial is crucial, and for urethral applications, softness, flexibility, and saturability are critical mechanical properties. Various synthetic biodegradable polymers, such as polylactide (PLA), polyglycolide (PGA), and poly-L-lactide-*co*-*e*-caprolactone (PLCL), have previously been studied.[4–8] However, plain PLA and PGA are relatively rigid and brittle for soft tissue engineering applications. Their mechanical properties could be tailored, for instance, by blending with softer and ductile biomaterials such as PLCL or polybutylene succinate (PBSu).[9,10] PBSu is a new aliphatic polyester in tissue engineering, and only few studies, mainly related to cartilage and bone tissue engineering, have been published.[11,12] The advantages of PBSu are its biodegradability, biocompatibility, and high flexibility, making it appealing also for soft tissue engineering applications.[11–13] However, to our knowledge, PBSu has previously not been studied for urethral tissue engineering.

The autologous human urothelial cells (hUC) have been the most abundantly studied cell type for urothelial regeneration and exhibited potential for urethral tissue engineering.[5,14,15] The isolation of autologous hUCs is feasible with bladder washing, which enables cell isolation, omitting the need of invasive biopsy.[16,17] However, in addition to the urothelium, the regeneration of a functional smooth muscle and connective tissue layer is at least equally important in reconstructing functional urethral tissue since the lack of smooth muscle layer may lead to overactive fibrosis and stenosis of the tissue-engineered graft.[18,19] In urological applications, the smooth muscle-derived progenitor cells are the most frequently studied cell type; however, the main problem in using autologous progenitor is the limited availability and donor site morbidity during cell isolation.[5,20,21] Though, human adipose-derived stromal cells (hASC) have been shown to differentiate into various cell types, including smooth muscle cells.[22,23] In addition, their potential mechanism of action may be related to stimulating local progenitor cells and angiogenesis, and inhibiting inflammatory processes.[22,24] Previously, implanting hASCs to a fibrous PLA mesh was shown to regenerate the smooth muscle layer and decrease the rate of urethral stenosis in rabbit urethra compared to PLA mesh only.[25] Thus hASCs are emerging as a potential cell type for smooth muscle regeneration.[5,25,26] The hASCs are abundantly available and easy to isolate, for instance, with liposuction, and due to their low immunogenicity, allogenic cells could also be considered for reconstruction.[26,27]

This study aimed to evaluate PLA/PBSu blend discs for urethral tissue engineering. The hUCs and hASCs viability, proliferation, phenotype, and gene expression were compared on 100/0 PLA/PBSu, 75/25 PLA/PBSu blend, 50/50 PLA/PBSu blend, and 0/100 PLA/PBSu discs. We hypothesized that PBSu would be beneficial for the hUCs and hASCs in in vitro cultures.

2 | MATERIALS AND METHODS

2.1 | Sample manufacturing

The polymer discs were made of medical grade poly(L/DL)lactide (PLA, L/DL ratio 70/30, Resomer LR 706S, Evonik Industries AG, Darmstadt, Germany) and commercial grade polybutylene succinate (PBSu, Bionolle 1020 MD, Showa Denko Europe GmbH, Munich, Germany). The inherent viscosity of the PLA was 4.0 dL/g, as stated by the manufacturer, and 1.1 dL/g for the PBSu, as measured by a viscometric analysis (Lauda PSV1, Lauda-Königshofen, Germany) with Ubbelohde capillaries (Schott-Instrument, Mainz, Germany) in chloroform at 25°C.

Before processing, the polymers were dried in a vacuum oven at 75°C for 8 h and let cool down to room temperature (RT). PLA and PBSu were extruded into rods using a custom-made co-rotating twin-screw extruder (Mini ZE 20*11.5 D, Neste Oy, Porvoo, Finland) in a nitrogen atmosphere. Four different types of rods (diameter approximately 2 mm) were manufactured: 100/0 PLA/PBSu (100/0), 0/100 PLA/PBSu (0/100), and two blends, 75/25 PLA/PBSu (75/25) containing 75 wt% of PLA and 25 wt% of PBSu and 50/50 PLA/PBSu (50/50) containing 50 wt% of PLA and 50 wt% PBSu.

To make the discs, the extruded rods were compression molded between metal plates (parameters in Table 1) into approximately 100 µm thick discs using a hot press (NIKE, Hydraulics Ab, Eskilstuna, Sweden). The discs were cut to samples with a diameter of 15 mm, washed with Aa Ethanol (Altia Oyj, Helsinki, Finland) in an ultrasonic bath, and dried for a couple of hours in a laminar hood followed by overnight in a vacuum. Before the cell studies, the discs were gamma sterilized (25 kGy, BBF Sterilisationsservice GmbH, Kernen, Germany). The cell culture plastic (polystyrene, PS; with hASC: Nunc, Thermo Fischer Scientific, MA, USA and with hUC: Sigma-Aldrich, Corning CellBIND®, St Louis, MO, USA) was used as a control.

2.2 | Initial characterization

For measuring the initial stiffness of the materials, the extruded rods were cut to 70 mm length, washed with Aa Ethanol (Altia Oyj) and gamma sterilized (25 kGy, BBF Sterilisationsservice GmbH, Kernen, Germany). The extruded and sterilized 2 mm diameter rods were tested by three-point bending at room temperature using an Instron 4411 material testing machine (Instron Ltd., High Wycombe, UK). The

TABLE 1 The compression molding parameters used in manufacturing the 100/0 PLA/PBSu, 75/25 PLA/PBSu, 50/50 PLA/PBSu, 0/100 PLA/PBSu discs for the study.

Material	100/0	75/25	50/50	0/100
Temperature (°C)	160	150	120	115
Pressure (MPa)	14	14	10	10
Time (s)	10	10	10	10

samples were immersed in phosphate buffered saline (PBS) for 1 h and blot dried before measuring their diameters and testing. The testing was conducted as described previously.[28] The bending span was 32 mm and the crosshead speed 5 mm/min. The bending modulus was calculated using the formula:

$$E = \frac{4 \times \text{slope} \times L^3}{3 \times \pi \times d^4} \times \frac{1}{1000},$$

where E = bending modulus (GPa), L = support span (mm), d = diameter of the rod (mm). The results are presented as averages of six measurements with the standard deviation.

Water contact angles of the discs were measured at RT by the sessile drop method in a video-based optical contact angle system (Theta Lite Optical Tensiometer, Biolin Scientific AB, Sweden) and OneAttension software. The measurements were carried out using deionized water, and the values were extracted via the tangent method. Average values were calculated from 12 parallel left and right angle results per sample (four samples per material, $n = 48$ per material).

The surface topographies of the discs were characterized by an atomic force microscope (AFM, XE-100, Park Systems, Santa Clara, USA). Three parallel areas of 5 μm × 5 μm per dry disc were scanned in a non-contact mode in air, using aluminum-coated silicon probes (ACTA, 37 N/m, 300 kHz, Applied Nano Structures Inc., Mountain View, USA). The average surface roughness (R_a and R_q) values were obtained by XEI image processing software (Park Systems, Santa Clara, USA).

2.3 | Cell isolation

2.3.1 | Urothelial cells

The hUCs were isolated as previously described[6,7] and the tissue samples were obtained from normal ureters of child donors during routine elective surgery in Tampere University Hospital, with the approval of the Ethics Committee of Pirkanmaa Hospital District (Tampere, Finland, R07160) and written consents from the parents. Briefly, the tissue pieces were cleaned, cut, and incubated overnight in a stripping solution containing 0.01% HEPES buffer (1 M, Sigma-Aldrich), 4×10^3% aprotinin (1 KIU/μL; Sigma-Aldrich), 0.1% EDTA (Sigma-Aldrich) and 0.01% penicillin/streptomycin (Lonza, Basel, Switzerland) in Hank's balanced salt solution (HBSS, Thermo Fischer) without Ca^{2+} and Mg^{2+} in order to loosen the urothelial layer. The urothelial sheets were separated from the stroma and digested in 0.1% trypsin (Lonza) for 30 min at 37°C in a shaking water bath. The trypsin was inactivated by adding 10% human serum (HS, Biowest, Nuaillé, France) to HBSS. The resulting suspension was centrifuged and resuspended in EpiLife medium (Thermo Fischer) supplemented with 1% of EpiLife defined growth supplement (EDGS; Thermo Fischer), 0.1% of $CaCl_2$ (Thermo Fischer), and 0.35% of antibiotics (100 U/μL penicillin and 0.1 mg/μL streptomycin, Lonza). The cells were cultured in EpiLife medium at 37°C in a humidified atmosphere with 5% CO_2. The hUCs from three donors in passages 3–4 were used in the experiments.

2.3.2 | Adipose stem stromal cells

The hASCs for the experiments were obtained from three different donors during elective surgery from Tampere University Hospital, with the approval of Ethics Committee of Pirkanmaa Hospital District (R15161) and patients' written consent. The hASCs were isolated using a mechanical and enzymatic isolation method as previously described.[29] Briefly, the adipose tissue sample was manually cut to smaller pieces, digested using collagenase NB 6 (SERVA Electrophoresis GmbH, Heidelberg, Germany), centrifuged, and filtered in sequential steps in order to separate the ASCs from the surrounding tissue. The isolated hASC were cultured in aMEM medium (Lonza) supplemented with 5% HS (Biowest) and 1% penicillin/streptomycin (Lonza) in T75 cell culture flasks (Thermo Fischer) in a humidified atmosphere with 5% of CO_2. Overall, hASCs from three donors in passages 2–3 were used in this study.

2.4 | Cell seeding

All the cell experiments were conducted in a 24-well plate format. The discs were placed at the bottoms of the wells and fixed with inserts (CellCrown24, Scaffdex Ltd, Tampere, Finland). The discs were preincubated in a medium for 24 h at 37°C before seeding approximately 20,000 hUCs or 2000 hASCs on each disc in a medium volume of 20 μL. The cells were allowed to adhere for 2 h, after which 1 mL of medium was carefully added to each well.

2.5 | Cell viability and proliferation

The viability of the hUCs and hASCs cultured on the different discs was assessed using a qualitative live/dead fluorescence staining (Thermo Fischer) after 7 and 14 days of culture. Briefly, the cells were incubated for 45 min at RT in a working solution containing 0.25 mM calcein AM (Thermo Fischer) and 0.3 mM ethidium homodimer-1 (EthD-1; Thermo Fischer). After the incubation, the cells were immediately imaged using a fluorescent microscope (IX51, Olympus, Tokyo, Japan).

The proliferation of hUCs and hASCs was assessed after 1, 7, and 14 days of culture by determining the DNA amount in the samples ($n = 9$) using a CyQUANT Cell Proliferation Assay kit (Thermo Fischer). Briefly, the cells were lysed with 0.1% Triton-X 100 lysis buffer (Sigma-Aldrich) and stored in −70°C until analysis. After one freeze–thaw cycle, 20 μL of each sample and 180 μL of a working solution containing CyQUANT GR dye and lysis buffer were pipetted to a 96-well plate. The fluorescence of three parallel samples was measured at 480/520 nm using a microplate reader (Victor 1420 Multilabel Counter; Wallac, Turku, Finland).

2.6 | Immunocytochemical stainings

Immunocytochemical stainings (Table 2) were used to evaluate the maintenance of the cytokeratin staining (AE1/AE3 pancytokeratin) of

TABLE 2 The primary and secondary antibodies used in immunocytochemical stainings.

Cells	Primary antibody	Dilution	Secondary antibody	Dilution
hUC	AE1/AE3 pancytokeratin (Thermo Scientific)	1:250	Alexa Fluor 488 (Life Technologies)	1:800
hASC	Alpha smooth muscle Actin (α-SMA; Abcam)	1:200	Alexa Fluor 488 (Life Technologies)	1:300
	Smooth muscle 22 alpha (SM22α; Abcam)	1:200	Alexa Fluor 488 (Life Technologies)	1:500
hUC and hASC	Vinculin (Invitrogen)		Alexa Fluor 488 (Life Technologies)	1:500
			Phalloidin-TRITC (Sigma-Aldrich)	1:500
			DAPI (Sigma-Aldrich)	1:2000

TABLE 3 The primer sequences used in quantitative real-time reverse transcription polymerase chain reaction.

Name		5′-sequence-3′	Product size (bp)	Accession number
Col I	Forward	CCAGAAGAACTGGTACATCAGCAA	94	NM_000088.3
	Reverse	CGCCATACTCGAACTGGAATC		
Col III	Forward	CAGCGGTTCTCCAGGCAAGG	179	NM_000090
	Reverse	CTCCACTGATCCCAGCAATCCC		
CK7	Forward	CATCGAGATCGCCACCTACC	80	NM_005556.3
	Reverse	TATTCACGGCTCCCACTCCA		
CK8	Forward	CCATGCCTCCAGCTACAAAAC	68	M34225.1
	Reverse	AGCTGAGGTTTTATTTTGGACC		
CK19	Forward	ACTACACGACCATCCAGGAC	80	NM_002276.4
	Reverse	GTCGATCTGCAGGACAATCC		
UPIa	Forward	GGGATCTCCAGTTGGTGG	80	NM_007000.3
	Reverse	TCTCAGCAAACAGGGACAGG		
UPIb	Forward	AGTCACCAAAACCTGGGACAG	64	NM_006952.3
	Reverse	TGATGGACCATTTACGCCACA		
RPLP0	Forward	AATCTCCAGGGGCACCATT	70	NM_001002
	Reverse	CGCTGGCTCCCACTTTGT		

hUCs, the differentiation potential of hASCs towards smooth muscle cells (α-SMA and SM22α), and actin cytoskeleton organization (phalloidin) after 7 and 14 days of cell culture. Additionally, the adhesion of the cells was assessed by staining the adhesion sites of the cells using vinculin combined with DAPI and phalloidin at 7 day time point.

Briefly, the cells were fixed with 4% paraformaldehyde supplemented with 0.2% Triton-X 100 for 15 min at RT and blocked with 1% bovine serum albumin (BSA). After fixing, the cells were incubated in primary antibody dilutions overnight at +4°C. The next day, the cells were incubated in the secondary antibody solutions diluted in 1% BSA for 45 min at +4°C. In order to see the actin cytoskeleton organization of the hASC, the cells were blocked overnight and incubated in 1:500 phalloidin-TRITC solution (Sigma-Aldrich) for 45 min at RT. Finally, the nuclei of all the cells were stained with DAPI (1:2000, Sigma-Aldrich). The cells were imaged immediately after staining using a fluorescent microscope (Olympus).

2.7 | Quantitative real-time polymerase chain reaction

The relative expression of collagen (Col) I, Col III, cytokeratin (CK) 7, CK8, CK19, uroplakin (UP) Ia, and UPIb genes was studied with quantitative real-time reverse transcription polymerase chain reaction (qRT-PCR). For the analysis, the hUCs and hASCs were cultured on 100/0, 75/25, 50/50, 0/100, and PS control until 14 day time point. Shortly, the total messenger RNA was isolated from the samples using Nucleospin RNA II kit (Macherey-Nagel, Düren, Germany) and then reverse transcribed to cDNA using High-Capacity cDNA Reverse Transcriptase Kit (Thermo Fischer Scientific). The reactions were conducted with an AbiPrism 7000 Sequence Detection System (Applied Biosystems) by initially activating the enzymes at 95°C for 10 min, followed by 45 cycles at 95°C for 15 s and 60°C for 60 s. The primer sequences (Immuno Diagnostic Oy, Hämeenlinna, Finland, and TAG Copenhagen A/S, Frederiksberg, Denmark) and the genes' accession numbers are gathered in Table 3. The qRT-PCR mixture contained cDNA, forward and reverse primers, and SYBR Green PCR Master Mix (Applied Biosystems). The data were normalized to the housekeeping gene RPLP0 (large ribosomal protein P0) expression with a previously described mathematical model.[30]

2.8 | Statistical analysis

The statistical analyses were performed with SPSS Statistics version 25 (IBM, Armonk, NY, USA). All quantitative data are presented as

averages with standard deviation (SD). The qRT-PCR and CyQuant analysis were repeated with three cell lines and three parallel samples with each material ($n = 9$). The contact angle measurements were performed for four parallel samples with at least 12 parallel measurements ($n = 48$). The bending modulus measurements were conducted for six parallel samples ($n = 6$). The statistical analysis for the bending modulus, qRT-PCR, and CyQuant data was done using non-parametric statistics with the Kruskal-Wallis test. For the contact angle measurements, the statistical analysis was done from the mean values of right and left angles using one-way ANOVA. The Bonferroni correction based on the number of the comparisons was used to minimize the error produced by familywise calculations. The results were considered statistically significant when the adjusted p value was <.05.

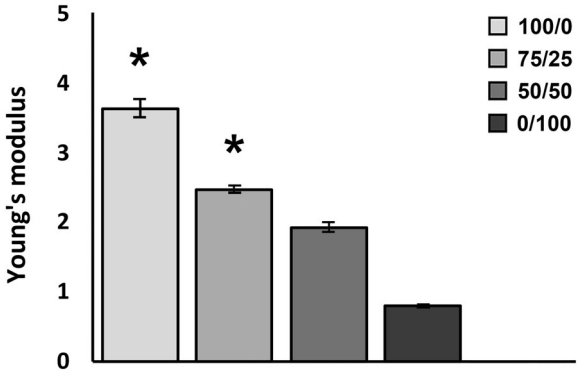

FIGURE 1 The initial bending modulus of 100/0 PLA/PBSu, 75/25 PLA/PBSu, 50/50 PLA/PBSu and 0/100 PLA/PBSu rods measured as sterile and wet. The stiffness of 100/0 and 75/25 was significantly higher compared to 0/100 (*p < .001 and <.05, respectively).

3 | RESULTS

3.1 | Initial material characterization

The influence of blending to the mechanical properties was assessed by measuring the bending modulus of the wet 100/0, 75/25, 50/50, and 0/100 rods. The stiffness of the materials decreased with increasing PBSu content (Figure 1). The bending modulus of 100/0 (PLA) was 3.9 GPa (p < .001 in comparison to 0/100 [PBSu]). Blending 25% of PBSu to PLA decreased the bending modulus by about one third (p < .05, with respect to 0/100) and blending 50% PBSu to PLA the stiffness was only about half of the stiffness of PLA (p < .05 with respect to 100/0).

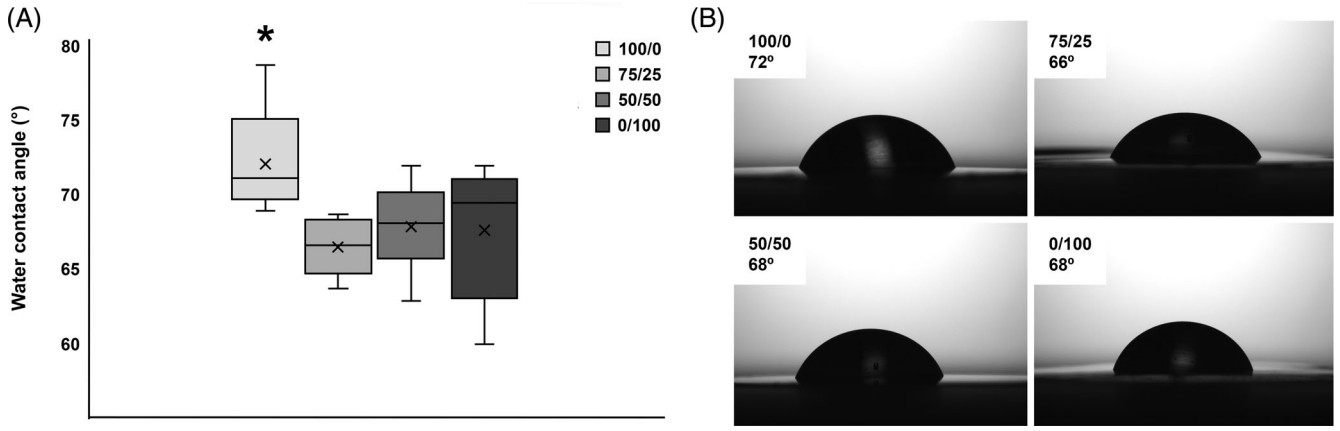

FIGURE 2 Water contact angle of 100/0 PLA/PBSu, 75/25 PLA/PBSu, 50/50 PLA/PBSu and 0/100 PLA/PBSu. (A) The water contact angle of 100/0 was significantly higher compared to all the other discs, *p < .001. (B) Selected images of water drops on the materials.

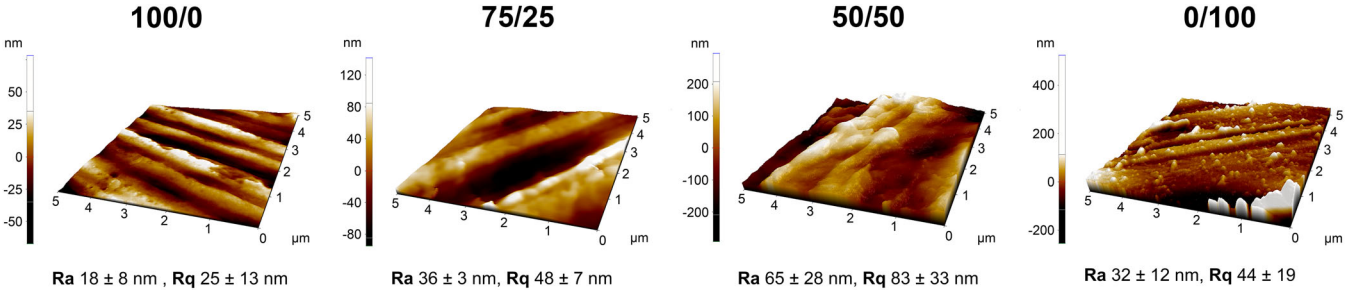

FIGURE 3 The initial surface roughness values of 100/0 PLA/PBSu, 75/25 PLA/PBSu, 50/50 PLA/PBSu and 0/100 PLA/PBSu measured with atomic force microscope.

The water contact angle was measured to assess the hydrophilicity of all the materials (Figure 2). 100/0 had a higher contact angle (72° ± 3°) compared to the PBSu-containing materials (75/25: 66° ± 2°, 50/50: 68° ± 3° and 0/100: 68° ± 4°, $p < .001$). There were no statistical differences between the PBSu-containing materials.

The initial surface roughness of the discs was assessed by imaging with AFM. The resulting images and corresponding surface roughness values are gathered in Figure 3. All the materials presented ridge-like structures. The surface roughness values of the discs were 18–65 R_a/nm (R_a) and 25–83 R_q/nm (R_q). Both the images and the R_a and R_q values suggest that 100/0 discs were slightly smoother than the PBSu-containing materials. Further, the surface roughness was measured after 14 days of incubation in medium, please see the Figure S1.

3.2 | Cell viability and proliferation

In order to evaluate the viability of the hUCs and hASCs cultured on the studied biomaterials, live/dead staining was conducted after 7 and 14 days (Figure 4).

The hUCs remained viable on all the materials (Figure 4A), and the number of dead cells was negligible. According to the quantitative proliferation assay, there were no significant differences in the hUC number at 1 day (Figure 5). After 7 days, 100/0 supported the proliferation of hUCs significantly better compared to 50/50 ($p < .05$) and 0/100 ($p < .001$). Further, the cell number on PS was significantly higher compared to 75/25 ($p < .05$), 50/50 ($p = .001$) and 0/100 ($p < .001$) after 7 days. At 14 day time point, PS supported the hUCs proliferation over all the other materials ($p < .001$). Additionally, 100/0 supported the hUCs proliferation significantly better than 50/50 ($p = .001$). The number of hUCs significantly increased between 1 and 7 days on all the materials except PS ($p < .001$). Between 7 and 14 day time points there was significant increase in the cell number only on PS ($p < .001$) and 0/100 ($p < .01$).

Further, the live/dead staining showed that all the materials containing PBSu supported the viability of hASCs throughout the whole 14 day culturing period, and only a few dead cells were detected (Figure 4B). Interestingly, 100/0 PLA/PBSu did not support the viability of hASCs. Instead of attaching and spreading on the material, the cells formed aggregates with each other. The weaker attachment of hASCs on 100/0 was also observed in the quantitative CyQUANT cell proliferation assay (Figure 6). The hASC number on 100/0 was significantly lower at all time points than the other materials ($p < .001$). The cell number significantly increased between 1 and 7 days on all the materials ($p < .001$), but not anymore between the 7 and 14 day time points, except on PS ($p < .05$). At the 14 day time point, the cell

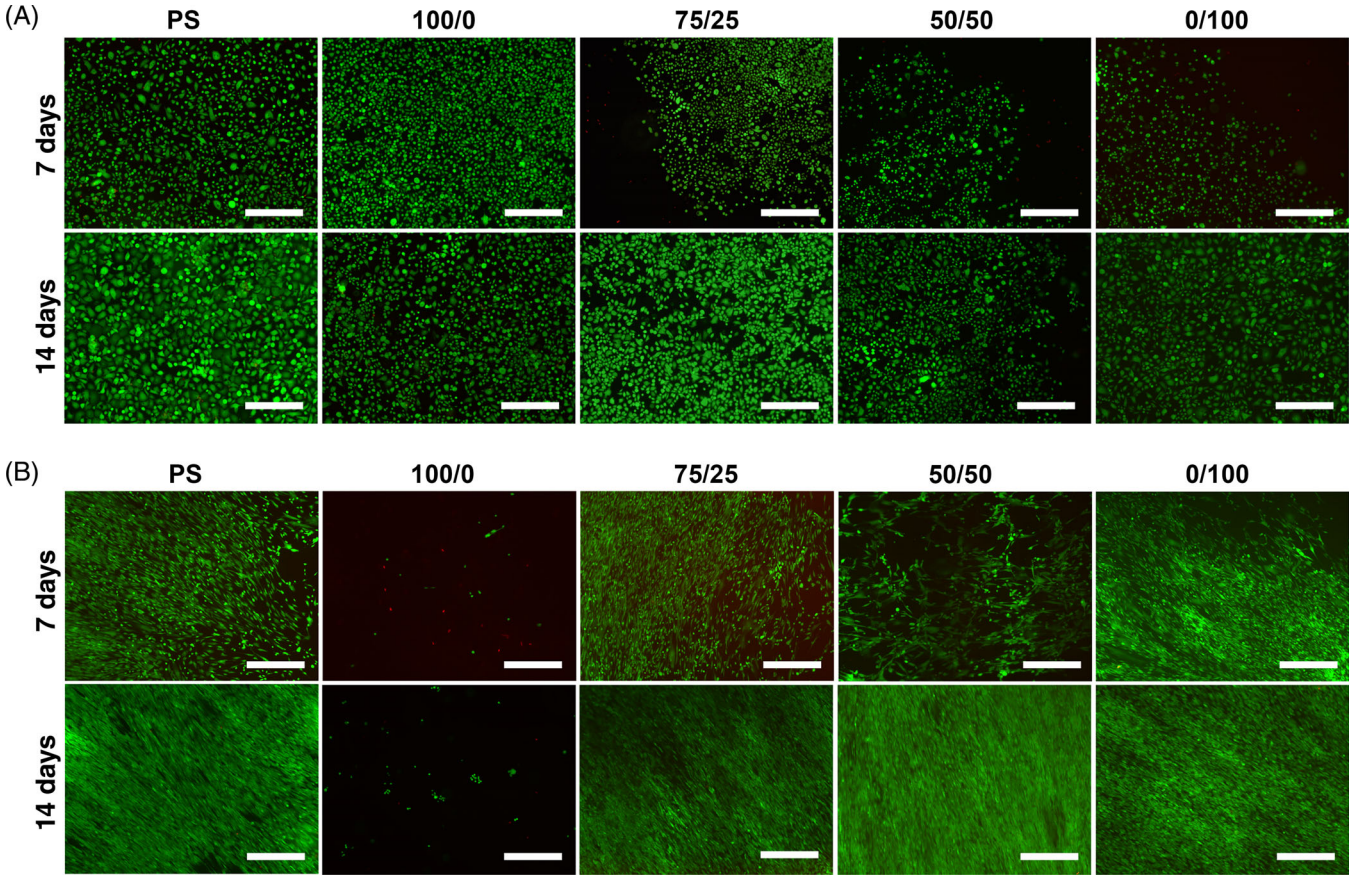

FIGURE 4 The viability of (A) hUCs and (B) hASCs cultured on control (PS), 100/0 PLA/PBSu, 75/25 PLA/PBSu, 50/50 PLA/PBSu and 0/100 PLA/PBSu after 7 and 14 days of cell culturing. Viable cells are stained green and dead cells red. Scale bar 500 μm.

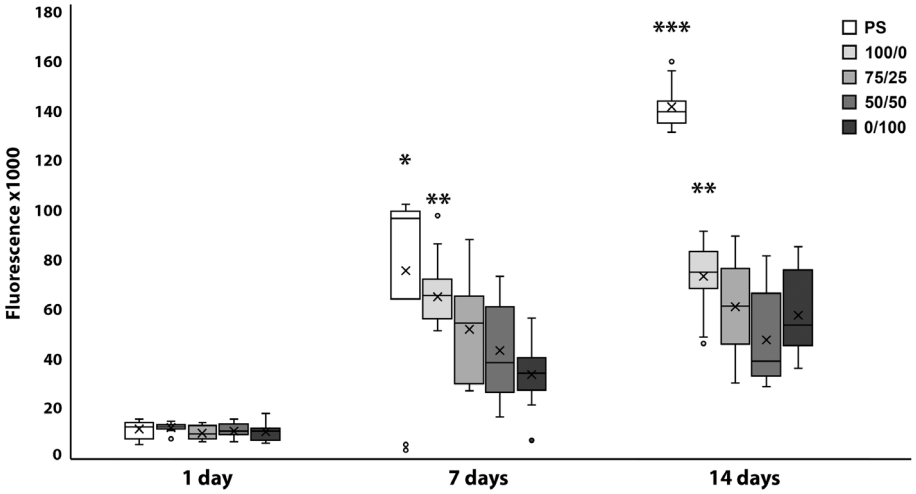

FIGURE 5 The proliferation of hUCs measured with CyQUANT cell proliferation assay kit on control polystyrene (PS), 100/0 PLA/PBSu, 75/25 PLA/PBSu, 50/50 PLA/PBSu and 0/100 PLA/PBSu after 1, 7, and 14 days of cell culturing. * PS was significantly better compared to 75/25 ($p < .05$), 50/50 ($p = .001$) and 0/100 ($p < .001$), ** 100/0 was significantly better compared to 0/100 (7 days, $p < .001$) and 50/50 (7 days; $p < .05$ and 14 days; $p < .001$). ***$p < .001$ with respect to all the other discs.

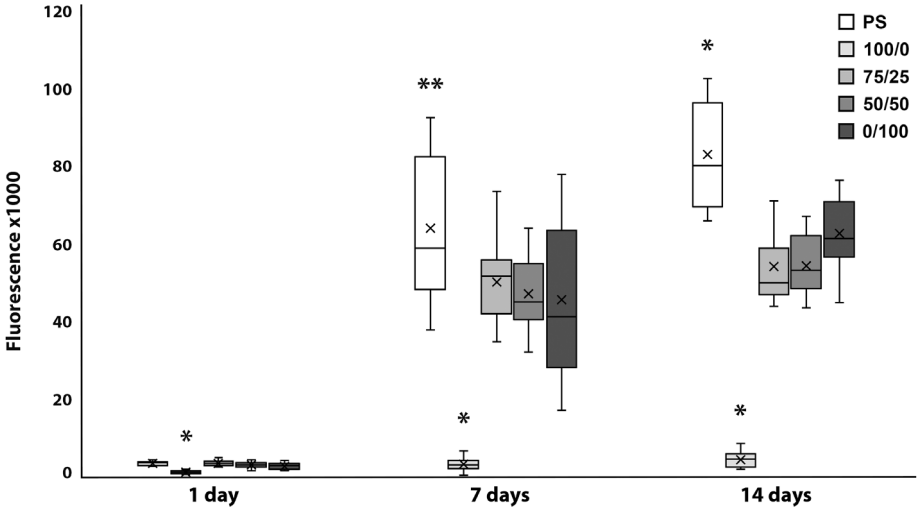

FIGURE 6 The proliferation of hASCs measured with CyQUANT cell proliferation Assay kit on control polystyrene (PS), 100/0 PLA/PBSu, 75/25 PLA/PBSu, 50/50 PLA/PBSu and 0/100 PLA/PBSu after 1, 7, and 14 days of cell culturing. * At all the time points 100/0 was significantly weaker compared to the other materials ($p < .001$) and at 14 day time point the PS was significantly better compared to the other materials (100/0, 75/25, 50/50: $p < .001$, PBSu: $p < .05$). **$p < .05$ with respect to 0/100.

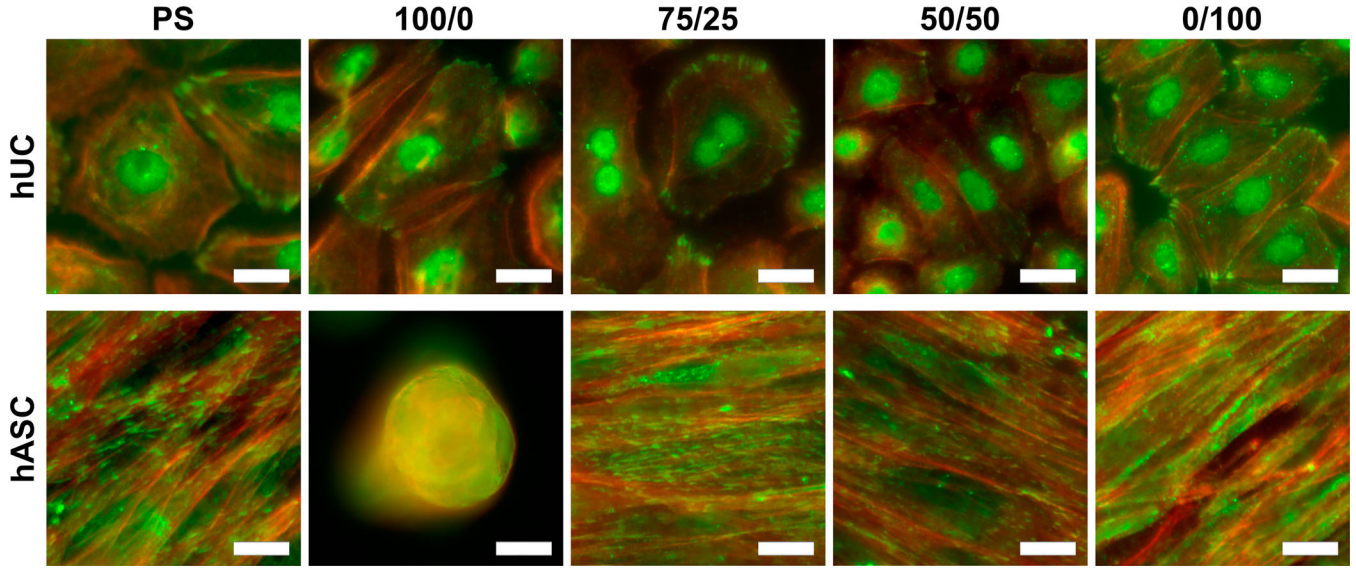

FIGURE 7 The attachment and actin cytoskeleton of hUCs and hASCs on control polystyrene (PS), 100/0 PLA/PBSu, 75/25 PLA/PBSu, 50/50 PLA/PBSu and 0/100 PLA/PBSu at 7 day time point. The actin cytoskeleton was stained red and focal adhesions were stained green with vinculin. The cell nuclei were stained blue with DAPI. Cell nuclei are shown green due to vinculin (green) and DAPI (blue) staining. For individual stainings, see Figures S2 and S3. Scale bar 20 μm.

number on PS was significantly higher compared to all the other materials (100/0, 75/25, 50/50: $p < .001$, 0/100: $p < .05$).

3.3 | Focal adhesion

The adhesion of hUCs and hASCs on PS, 100/0, 75/25, 50/50, and 0/100 was qualitatively assessed with vinculin staining, indicating the focal adhesions of the cells. Based on qualitative evaluation, the hUCs focal adhesion points seemed equal on discs compared to the CellBIND® polystyrene control and the most intensive vinculin staining was detected as small points on the cells' edges. Additionally, the focal adhesion points were also distributed throughout hUC cell membranes and under the nuclei. The focal adhesion points in hASCs were evenly spread throughout the cells (Figure 7). According to visual analysis, the staining of focal adhesion points was equally intensive in all PBSu-containing materials and the intensity was equal to the PS control. Further, the focal points were almost nonvisible on the hASC aggregates on 100/0.

3.4 | Phenotype maintenance of hUCs and smooth muscle differentiation of hASCs

The maintenance of the hUCs phenotype was evaluated with pancytokeratin (AE1/AE3) staining. The hUCs intensively stained with pancytokeratin at 7 and 14 day time points (Figure 8). According to the visual analysis, there were no distinctive differences between the time points or studied materials, indicating that all the materials supported the hUCs phenotype equally. Additionally, on all the materials, the hUCs seemed to have normal urothelial morphology, and no changes in the cell morphology were detected during the evaluation period.

The immunocytochemical staining with phalloidin revealed that the hASC grow aligned on the PBSu-containing discs. Additionally the

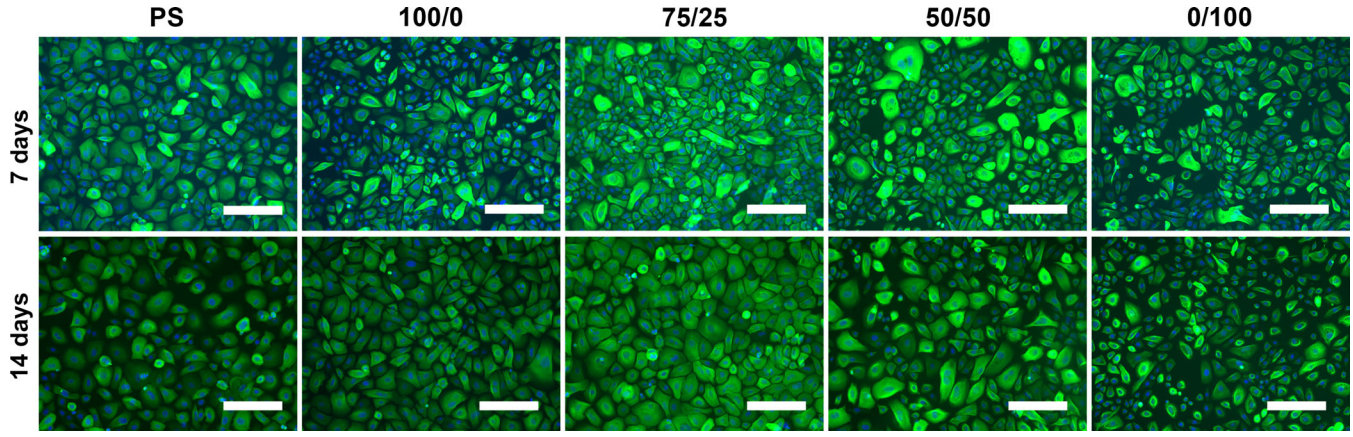

FIGURE 8 The pancytokeratin staining of the hUCs at 7 and 14 day time points cultured on control PS, 100/0 PLA/PBSu, 75/25 PLA/PBSu, 50/50 PLA/PBSu and 0/100 PLA/PBSu. The green fluorescence demonstrates the pancytokeratin (AE1/AE3) staining and the cell nuclei are stained with DAPI (blue fluorescence). Scale bar 200 μm.

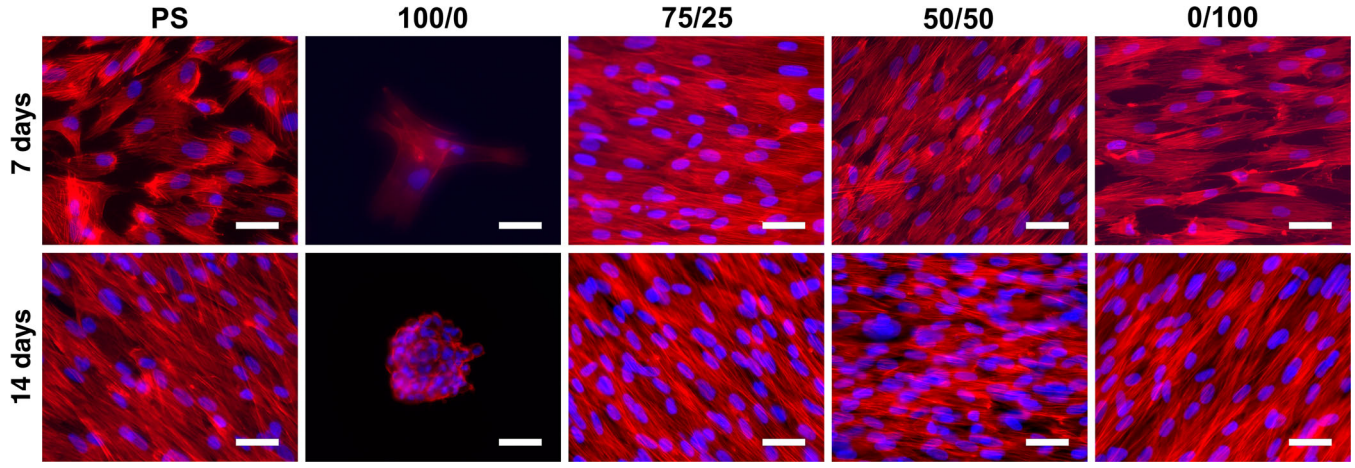

FIGURE 9 The cytoskeleton organization of hASC cultured on control PS, 100/0 PLA/PBSu, 75/25 PLA/PBSu, 50/50 PLA/PBSu and 0/100 PLA/PBSu after 7 and 14 days of cell culturing. The actin cytoskeleton was stained with phalloidin (red) and the cell nuclei were stained with DAPI (blue). Scale bar 50 μm.

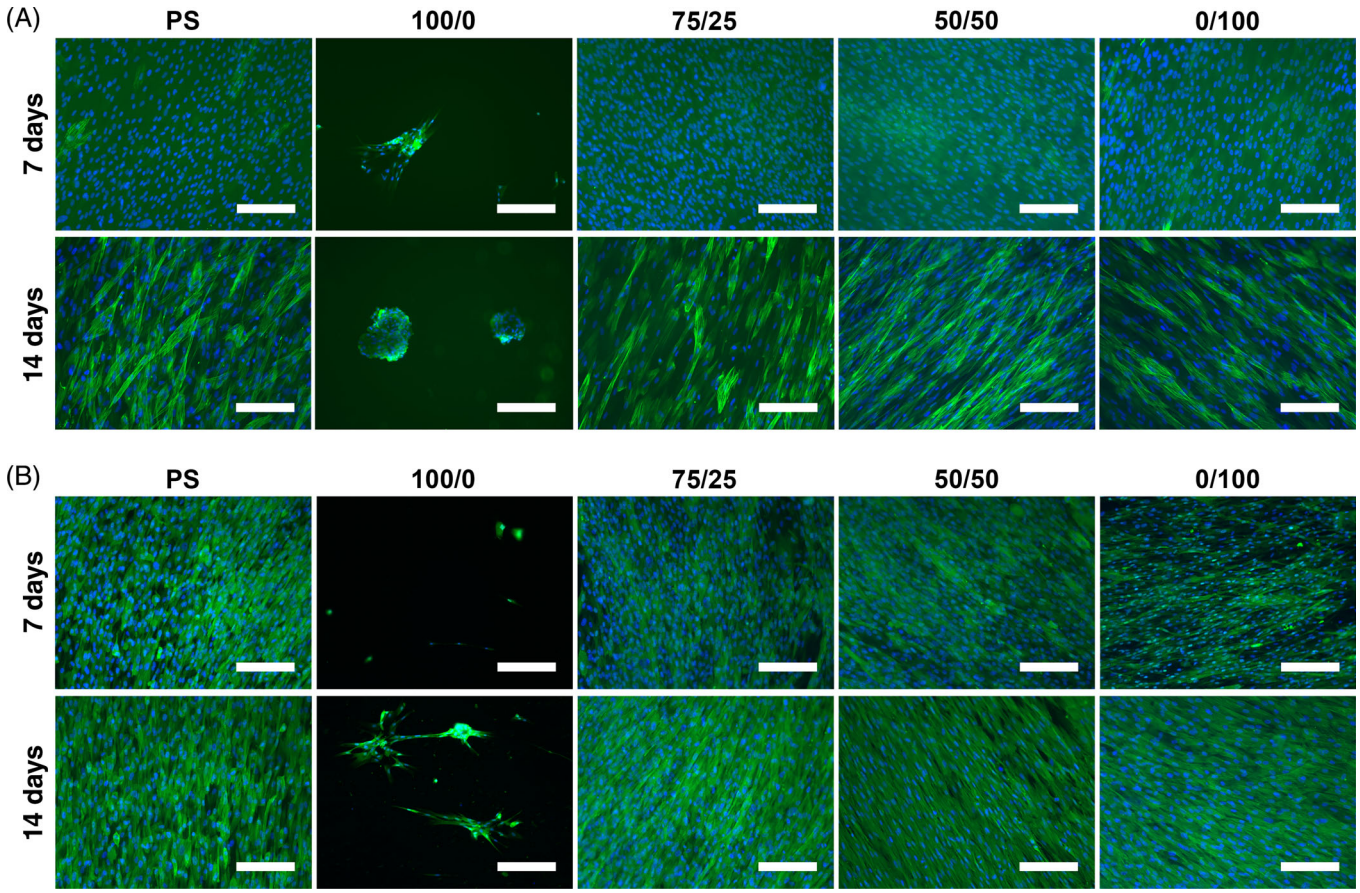

FIGURE 10 (A) α-SMA and (B) SM22α staining of hASCs cultured on control PS, 100/0 PLA/PBSu, 75/25 PLA/PBSu, 50/50 PLA/PBSu and 0/100 PLA/PBSu for 7 and 14 days. The green fluorescence is representing α-SMA and SM22α staining and cell nuclei are stained blue with DAPI. Scale bar 200 μm.

cytoskeletons of hASCs on the PBSu-containing discs were organized and aligned after 7 and 14 days of culture (Figure 9), and based on qualitative evaluation, no distinctive differences were detected compared to PS. However, in the hASC aggregates on 100/0, the cytoskeleton was not as organized due to a spherical cell morphology.

Additionally, the staining of smooth muscle cell markers α-SMA and SM22α in hASCs was studied after 7 and 14 days (Figure 10). The materials seemed to support the staining of α-SMA on cultured hASCs (Figure 10A). Additionally, based on the qualitative assessment, the intensity of α-SMA staining increased between 7 and 14 day time points on all the materials except 100/0. SM22α (Figure 10B) staining was intensive on all PBSu-containing materials and no apparent differences between them were detected.

3.5 | Real-time quantitative polymerase chain reaction

The hUCs expression of CK7, CK8, CK19, UPIa, and UPIb and hASCs expression of collagen (Col) I and Col III were studied after 14 days of cell culture on PS, 100/0, 75/25, 50/50, and 0/100 (Figures 11, 12).

There were no statistical differences in the expression of CK7, CK19, UPIa, and UPIb. However, hUCs cultured on control PS expressed CK8 significantly more than 50/50 ($p < .05$). The hASCs expressed both Col I and Col III. The expression of Col I was significantly higher on 50/50 ($p < .05$) and PS ($p < .001$) compared to 100/0. There were no significant differences between the materials in Col III expression.

4 | DISCUSSION

Surgical repair of urethral defects is highly challenging and susceptible to complications. New treatment options are needed and tissue engineering aims to provide a novel solution for urethral reconstruction. In addition to utilizing optimal cell types for urethral reconstruction, the main target for development is related to biomaterial selection. The biomaterial for urethral tissue engineering should be biocompatible, soft, flexible, easy to form as a tubular structure, and sustain suturing. Moreover, the biomaterial should support the urothelial and smooth muscle regeneration and degrade while the urethral tissue is restored. Although various synthetic biomaterials are already studied, developing an optimal biomaterial yet requires extensive research.[5,20,31] We

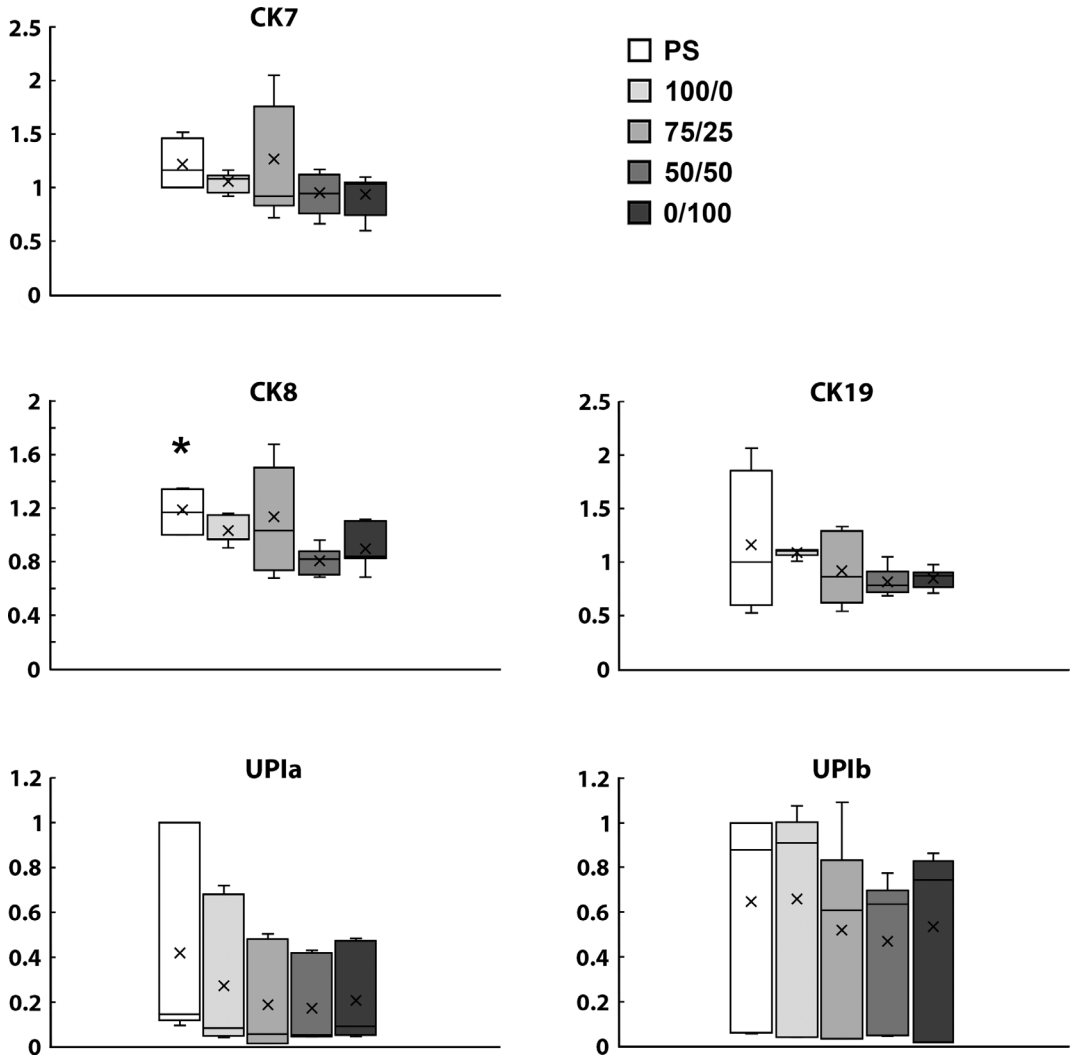

FIGURE 11 The expression of markers CK7, CK8, CK19, UPIa and UPIb were evaluated after 14 days of culture with hUCs cultured on control PS, 100/0 PLA/PBSu, 75/25 PLA/PBSu, 50/50 PLA/PBSu and 0/100 PLA/PBSu. *$p < .05$ with respect to 50/50.

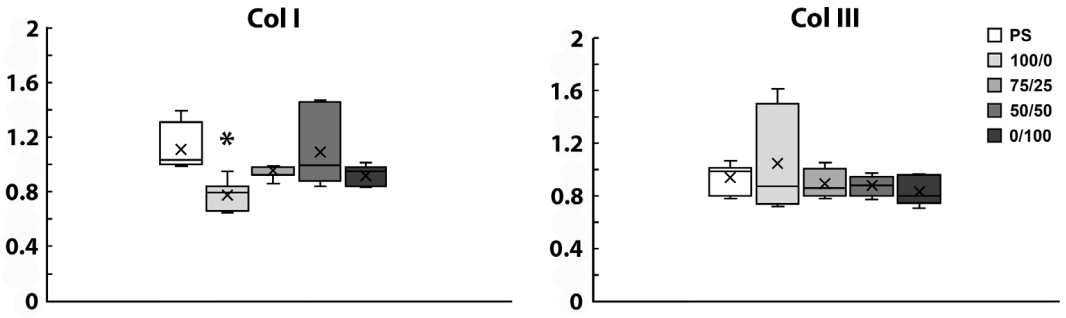

FIGURE 12 The expression of markers Col I and Col III were evaluated after 14 days of culture with hASCs cultured on control PS, 100/0 PLA/PBSu, 75/25 PLA/PBSu, 50/50 PLA/PBSu and 0/100 PLA/PBSu. * with respect to PS ($p < .001$) and 50/50 ($p < .05$).

compared the 100/0 PLA/PBSu (100/0), 75/25 PLA/PBSu (75/25), 50/50 PLA/PBSu (50/50) and 0/100 PLA/PBSu (0/100) for the viability, proliferation, adhesion, and phenotype maintenance of hUCs and hASCs. Further, the hASCs differentiation towards smooth muscle cells was evaluated. To our knowledge, this is the first study where PBSu and PLA/PBSu blends have been studied and compared to PLA for urethral tissue engineering.

PBSu has previously been utilized in biodegradable packaging materials, whereas the interest in studying PBSu in medical applications and tissue engineering has recently arisen. PBSu is biocompatible, easy

to process, elastic and flexible, and therefore appealing for urethral applications. Previously, the cell compatibility of PBSu has been studied with ASCs, bone marrow stem cells and mouse fibroblasts in vitro.[12,32,33] These results are in line with our current results on hUCs and hASCs viability and proliferation, further indicating a good cell compatibility of the PBSu. Blending PBSu with other polyesters, like PLA, allows tailoring of the mechanical properties resulting in more ductile, soft, and hydrophilic biomaterial compared to plain PLA.[13,34,35] To assess the influence of increasing PBSu content to the stiffness of the materials, we measured the bending modulus of the 100/0, 75/25, 50/50 and 0/100 rods. The rods were tested wet, after 1 h immersion in PBS. We showed that, 25% addition of PBSu decreased the stiffness of the material by one third and 50% addition by half, compared to 100/0. These results are consistent with the previous studies, which demonstrate decreasing Young's modulus with increasing PBSu content in PLA/PBSu blends. Even though the stiffness of the rods is not directly comparable to the properties of the discs, these results show the effect of blending PLA with PBSu.[36–40] In our surface characterization of the 100/0, 75/25, 50/50 and 0/100 discs, we showed that the 100/0 had a higher contact angle compared to the PBSu-containing materials. Our results are concordant with previous study by Wang et al. demonstrating that blending PBSu to PLA decreases the contact angle compared to plain PLA resulting in a more hydrophilic blend.[41] PBSu is slightly more hydrophilic than PLA and even a 25 wt% addition of PBSu into PLA improves the hydrophilicity of the blend. Additionally, our initial surface roughness results showed that 100/0 was smoother compared to the PBSu-containing materials and that the discs presented ridge-like surface patterns due to the manufacturing method, which might be one factor leading to better cell attachment.[6,7,42,43] Moreover, Kun et al. have demonstrated that PBSu and PBSu/PLA blends induced only mild tissue reaction and no extensive fibrosis was detected in in vivo biocompatibility evaluation,[32] which also supports the results of our study demonstrating good in vitro cell compatibility of PBSu-containing discs.

The hUCs are the most abundantly studied cell type for urothelial regeneration in urethral tissue engineering and the hUCs are well known to maintain their viability on various synthetic biomaterials as PLA, PLCL and PGA.[6,7,14,44] This is further illustrated in our study, where we showed excellent viability of hUCs on all the studied biomaterials. The hUCs remained viable during the whole 14 day assessment period, and hardly any dead cells were visible. In addition, there were no distinctive differences on focal adhesion marker staining of hUCs cultured on different discs or CellBIND® control PS, which further indicates similar adhesion of hUCs on all the studied materials. In hUCs, the vinculin staining was detected throughout the cell areas and also under the cell nuclei. The latter might also be caused by an unspecific antibody binding to a protein structurally similar to vinculin in hUC.[45,46] This kind of staining was not detected in hASC. Additionally, at least to our knowledge, the staining of focal adhesion markers has not been previously reported with hUCs cultured on biodegradable polymers.

The hUCs proliferated well on all the studied discs, and there were no significant differences on hUCs number between 100/0, 75/25, or 0/100 discs at 14 day time point. However, there were fewer hUCs on 50/50 than 100/0 or PS after 14 days of cell culturing. In addition, we evaluated the phenotype maintenance of hUCs with immunostaining of AE1/AE3 pancytokeratin and quantitative gene expression of cytokeratin (CK) 7, CK8, CK19, uroplakin (UP) Ia, and UPIb. The CKs are a cluster of intermediate filament proteins widely expressed in different epithelial tissues, including urothelium. The UPs, on the other hand, are transmembrane proteins mainly present in the mature superficial urothelial cells. These proteins have widely been used to characterize and follow the phenotype maintenance of urothelial cells in vitro and in vivo.[6,8,47–49] Our results demonstrated no apparent differences in hUCs pancytokeratin staining intensity between the biomaterials or time points. Additionally, no statistical differences in the expression of the above-described genes were found between the studied biomaterials, indicating that they support the hUCs phenotype during the 14 day culturing period. We have previously shown that hUCs retain their urothelial potential on PLCL based biomaterials in in vitro cell cultures, and these results further verify the hUCs capability to maintain their phenotype when cultured on synthetic biomaterials. At least to our knowledge, no previous results on hUCs adhesion, viability, proliferation, or phenotype maintenance on PBSu-containing biomaterials have been published.

Interestingly, the viability, attachment, and proliferation of hASCs were poor on 100/0 discs, and PBSu undeniably improved the hASCs compatibility on the different discs. On 100/0, the hASCs did not proliferate, but formed aggregates, and preferred attaching to each other instead of the biomaterial surface. This might be partly due to the lower hydrophilicity, the higher stiffness, or the smoother surface of the PLA compared to the PBSu-containing materials.[11,50] On the PBSu-containing discs, the hASCs proliferated well and based on cell live/dead imaging or cell proliferation no distinctive differences were detected relative to the PBSu concentration. Previously, Ojansivu et al. studied PBSu for bone tissue engineering, demonstrating that the hASCs proliferated significantly better on PBSu-containing 3D knitted scaffolds than plain PLA scaffolds and hASCs in PLA scaffolds formed cell clusters, which are concordant with the results in this study.[33] Further, the staining of focal adhesion marker was distinctively higher on PBSu-containing discs than 100/0, where hardly any focal adhesion markers were detected. Foldberg et al. have also demonstrated the ASCs cultured on PLA films represented very few focal adhesions, additionally, the number of ASCs was significantly lower on both flat and patterned PLA films compared to PS.[51] Similarly to Foldberg et al, in our study based on visual qualitative assessment, the focal adhesion markers were more abundantly detected in hASCs cultured on PBSu-containing materials compared to 100/0. The hASC cytoskeleton organization was evaluated with phalloidin staining on the different materials. The staining indicated that the hASCs on PBSu-containing biomaterials grew aligned to adjacent cells and the cytoskeleton was well organized and aligned parallel with elongated cell morphology as in control PS. However, on 100/0, the hASCs were spherical and organization of the cytoskeleton was not visible. The hASCs formed clusters on 100/0, indicating poor attachment, as demonstrated previously,[33] whereas the results of our study demonstrate

good cell compatibility of PBSu-containing biomaterials. Our results illustrated that the hASCs cultured on PBSu-containing biomaterials stained with smooth muscle markers α-SMA and SM22α equally to the control and superior to 100/0.[52,53] The hASCs were stained with α-SMA and SM22α markers both at 7 and 14 day time points, indicating ability to support smooth muscle cell-like phenotype of hASCs on all PBSu-containing discs. Previously, it has been published that PBSu might aid osteogenic differentiation of hASCs.[33] However, at least to our knowledge, this is the first study demonstrating that the hASCs preserve their potential for smooth muscle differentiation when cultured on PBSu-containing materials. Since smooth muscle layer regeneration is crucial for the reconstruction of functional urethral tissue, the results of this study are highly encouraging for PBSu in urethral applications.

5 | CONCLUSION

This is the first study to evaluate PBSu-containing biomaterials for urethral tissue engineering to the best of our knowledge. PBSu-containing discs were more hydrophilic than 100/0 and supported the viability, proliferation and phenotype maintenance of both hASCs and hUCs. The hUCs remained viable and proliferated on all the studied materials. The cells also maintained their epithelial phenotype during the 14-day culturing period. Moreover, all the materials containing PBSu promoted the viability and proliferation of hASC, whereas 100/0 did not. The PBSu-containing discs also appeared to maintain the hASCs differentiation capability towards smooth muscle cells, being highly beneficial in urothelial applications.

ACKNOWLEDGMENTS

The authors want to thank Alma Kurki, Anna-Maija Honkala, Miia Juntunen, Sari Kalliokoski, Suvi Heinämäki and Heikki Liejumäki for their excellent technical assistance. The author want to thank also Tuija Lahdes-Vasama and Minna Kelloniemi for providing tissues for cell isolation for this study. Further, the Tampere Imaging Facility, Biomeditech, Faculty of Medicine and Health Technologies, Tampere University is acknowledged for the service.

FUNDING INFORMATION

This research was funded by the Competitive Research Funding of the Pirkanmaa Hospital District (9AB069), Academy of Finland (312413/SM, 339405/RS), TAU graduate school, The Finnish Medical Foundation (3856) and the Finnish Foundation for Technology Promotion.

CONFLICT OF INTEREST STATEMENT

The authors declare no conflict of interest.

DATA AVAILABILITY STATEMENT

The research data will be available from the corresponding author upon request.

REFERENCES

1. Baskin LS, Ebbers MB. Hypospadias: anatomy, etiology, and technique. *J Pediatr Surg*. 2006;41:463-472.
2. Yamzon J, Perin L, Koh CJ. Current status of tissue engineering in pediatric urology. *Curr Opin Urol*. 2008;18:404-407.
3. Mangir N, Roman S, Macneil S. Improving the biocompatibility of biomaterial constructs and constructs delivering cells for the pelvic floor. *Curr Opin Urol*. 2019;29:419-425.
4. Pariente JL, Kim BS, Atala A. In vitro biocompatibility assessment of naturally derived and synthetic biomaterials using normal human urothelial cells. *J Biomed Mater Res*. 2001;55:33-39.
5. De Kemp V, De Graaf P, Fledderus JO, Bosch JLHR, De Kort LMO. Tissue engineering for human urethral reconstruction: systematic review of recent literature. *PLoS One*. 2015;10:1-14.
6. Sartoneva R, Haaparanta AM, Lahdes-Vasama T, et al. Characterizing and optimizing poly-L-lactide-co-epsilon-caprolactone membranes for urothelial tissue engineering. *J Royal Soc Interface R Soc*. 2012;9:3444-3454.
7. Sartoneva R, Haimi S, Miettinen S, et al. Comparison of a poly-L-lactide-co-ε-caprolactone and human amniotic membrane for urothelium tissue engineering applications. *J R Soc Interface*. 2011;8:671-677.
8. Sartoneva R, Nordback PH, Haimi S, et al. Comparison of poly(l-lactide-co-varepsilon-caprolactone) and poly(trimethylene carbonate) membranes for urethral regeneration: an In vitro and In vivo study. *Tissue Eng Part A*. 2017;24:117-127.
9. Shen S, Rodion K, Tolga Sengül KS. Polylactide (PLA) and its blends with poly(butylene). *Polymers*. 2019;11:1-21.
10. Nair LS, Laurencin CT. Biodegradable polymers as biomaterials. *Prog Polym Sci*. 2007;32:762-798.
11. Li H, Chang J, Cao A, Wang J. In vitro evaluation of biodegradable poly(butylene succinate) as a novel biomaterial. *Macromol Biosci*. 2005;5:433-440.
12. Coutinho DF, Gomes ME, Neves NM, Reis RL. Development of micropatterned surfaces of poly(butylene succinate) by micromolding for guided tissue engineering. *Acta Biomater*. 2012;8:1490-1497.
13. Almeida LR, Martins AR, Fernandes EM, et al. New biotextiles for tissue engineering: development, characterization and in vitro cellular viability. *Acta Biomater*. 2013;9:8167-8181.
14. Pariente JL, Kim BS, Atala A. In vitro biocompatibility evaluation of naturally derived and synthetic biomaterials using normal human bladder smooth muscle cells. *J Urol*. 2002;167:1867-1871.
15. Fossum M, Svensson J, Kratz G, Nordenskjold A. Autologous in vitro cultured urothelium in hypospadias repair. *J Pediatr Urol*. 2007;3:10-18.
16. Fossum M, Nordenskjold A. Tissue-engineered transplants for the treatment of severe hypospadias. *Horm Res Paediatr*. 2010;73:148-152.
17. Nagele U, Maurer S, Feil G, et al. In vitro investigations of tissue-engineered multilayered urothelium established from bladder washings. *Eur Urol*. 2008;54:1414-1422.
18. Horst M, Madduri S, Gobet R, et al. Engineering functional bladder tissues. *J Tissue Eng Regen Med*. 2013;7:515-522.
19. Orabi H, AbouShwareb T, Zhang Y, Yoo JJ, Atala A. Cell-seeded tubularized scaffolds for reconstruction of long urethral defects: a preclinical study. *Eur Urol*. 2013;63:531-538.
20. Orabi H, Bouhout S, Morissette A, Rousseau A, Chabaud S, Bolduc S. Tissue engineering of urinary bladder and urethra: advances from bench to patients. *Sci World J*. 2013;2013:1-13.
21. Raya-Rivera AM, Esquiliano D, Fierro-Pastrana R, et al. Tissue-engineered autologous vaginal organs in patients: a pilot cohort study. *Lancet*. 2014;384:329-336.
22. Patrikoski M, Mannerström B, Miettinen S. Perspectives for clinical translation of adipose stromal/stem cells. *Stem Cells Int*. 2019;2019:16-18.
23. Lindroos B, Aho KL, Kuokkanen H, et al. Differential gene expression in adipose stem cells cultured in allogeneic human serum versus fetal bovine serum. *Tissue Eng Part A*. 2010;16:2281-2294.

24. Kuismanen K, Sartoneva R, Haimi S, et al. Autologous adipose stem cells in treatment of female stress urinary incontinence: results of a pilot study. *Stem Cells Transl Med*. 2014;3:936-941.
25. Wang DJ, Li MY, Huang WT, et al. Repair of urethral defects with polylactid acid fibrous membrane seeded with adipose-derived stem cells in a rabbit model. *Connect Tissue Res*. 2015;56:434-439.
26. Jack GS, Almeida FG, Zhang R, Alfonso ZC, Zuk PA, Rodríguez LV. Processed lipoaspirate cells for tissue engineering of the lower urinary tract: implications for the treatment of stress urinary incontinence and bladder reconstruction. *J Urol*. 2005;174:2041-2045.
27. Lindroos B, Suuronen R, Miettinen S. The potential of adipose stem cells in regenerative medicine. *Stem Cell Rev*. 2011;7:269-291.
28. Niemelä T, Niiranen H, Kellomäki M, Törmälä P. Self-reinforced composites of bioabsorbable polymer and bioactive glass with different bioactive glass contents. Part I: initial mechanical properties and bioactivity. *Acta Biomater*. 2005;1:235-242.
29. Kyllönen L, Haimi S, Mannerström B, et al. Effects of different serum conditions on osteogenic differentiation of human adipose stem cells in vitro. *Stem Cell Res Ther*. 2013;4:17.
30. Pfaffl MW. A new mathematical model for relative quantification in real-time RT-PCR. *Nucleic Acids Res*. 2001;29:e45.
31. Qi N, Li WJ, Tian H. A systematic review of animal and clinical studies on the use of scaffolds for urethral repair. *J Huazhong Univ Sci Technol*. 2016;36:111-117.
32. Kun H, Wei Z, Xuan L, Xiubin Y. Biocompatibility of a novel poly(butyl succinate) and polylactic acid blend. *ASAIO J*. 2012;58:262-267.
33. Ojansivu M, Johansson L, Vanhatupa S, et al. Knitted 3D scaffolds of polybutylene succinate support human mesenchymal stem cell growth and osteogenesis. *Stem Cells Int*. 2018;2018:1-11.
34. Shi K, Bai Z, Su T, Wang Z. Selective enzymatic degradation and porous morphology of poly(butylene succinate)/poly(lactic acid) blends. *Int J Biol Macromol*. 2019;126:436-442.
35. Ribeiro VP, Almeida LR, Martins AR, et al. Modulating cell adhesion to polybutylene succinate biotextile constructs for tissue engineering applications. *J Tissue Eng Regen Med*. 2017;11:2853-2863.
36. Kimble LD, Bhattacharyya D, Kimble LD, Bhattacharyya D. In vitro degradation effects on strength, stiffness, and creep of PLLA/PBS: A potential stent material. *Int J Polym Mater Polym Biomater*. 2015;4037:299-310.
37. Deng Y, Thomas NL. Blending poly(butylene succinate) with poly(lactic acid): ductility and phase inversion effects. *Eur Polym J*. 2015;71:534-546.
38. Zhao P, Liu W, Wu Q, Ren J. Preparation, mechanical, and thermal properties of biodegradable polyesters/poly(lactic acid) blends. *J Nanomater*. 2010;2010:1-8.
39. Delamarche E, Mattlet A, Livi S, Gérard JF, Bayard R, Massardier V. Tailoring biodegradability of poly(butylene succinate)/poly(lactic acid) blends with a deep eutectic solvent. *Front Mater*. 2020;7:1-13.
40. Shibata M, Inoue Y, Miyoshi M. Mechanical properties, morphology, and crystallization behavior of blends of poly(l-lactide) with poly(butylene succinate-co-l-lactate) and poly(butylene succinate). *Polymer*. 2006;47:3557-3564.
41. Wang Y, Xiao Y, Duan J, Yang J, Wang Y, Zhang C. Accelerated hydrolytic degradation of poly(lactic acid) achieved by adding poly(butylene succinate). *Polym Bull*. 2015;73:1067-1083.
42. Lampin M, Warocquier-Clérout R, Legris C, Degrange M, Sigot-Luizard MF. Correlation between substratum roughness and wettability, cell adhesion, and cell migration. *J Biomed Mater Res*. 1997;36:99-108.
43. Ma Z, Mao Z, Gao C. Surface modification and property analysis of biomedical polymers used for tissue engineering. *Colloids Surfaces B: Biointerfaces*. 2007;60:137-157.
44. Eberli D, Filho LF, Atala A, Yoo JJ. Composite scaffolds for the engineering of hollow organs and tissues. *Methods*. 2009;47:109-115.
45. Quinlan MP. Vinculin, VASP, and profilin are coordinately regulated during Actin remodeling in epithelial cells, which requires de novo protein synthesis and protein kinase signal transduction pathways. *J Cell Physiol*. 2004;200:277-290.
46. Lüthje P, Brauner H, Ramos NL, et al. Estrogen supports urothelial defense mechanisms. *Sci Trans Med*. 2013;5:190ra80.
47. Apodaca G. The uroepithelium: not just a passive barrier. *Traffic*. 2004;5:117-128.
48. Southgate J, Masters JRW, Trejdosiewicz LK. In: Freshney RI, Freshney MG, eds. *Culture of Human Urothelium*. John Wiley & Sons, Inc.; 2002:381-399. doi:10.1002/0471221201.ch12
49. Amesty MV, Chamorro CI, López-Pereira P, et al. Creation of tissue-engineered urethras for large urethral defect repair in a rabbit experimental model. *Front Pediatr*. 2021;9:1-9.
50. Webb K, Hlady V, Tresco PA. Relative importance of surface wettability and charged functional groups on NIH 3T3 fibroblast attachment, spreading, and cytoskeletal organization. *J Biomed Mater Res*. 1998;41:422-430.
51. Foldberg S, Petersen M, Fojan P, et al. Patterned poly(lactic acid) films support growth and spontaneous multilineage gene expression of adipose-derived stem cells. *Colloids Surf B: Biointerfaces*. 2012;93:92-99.
52. Lu SH, Lin ATL, Chen KK, Chiang HS, Chang LS. Characterization of smooth muscle differentiation of purified human skeletal muscle-derived cells. *J Cell Mol Med*. 2011;15:587-592.
53. Solway J, Seltzer J, Samaha FF, et al. Structure and expression of a smooth muscle cell-specific gene, SM22α. *J Biol Chem*. 1995;270:13460-13469.

SUPPORTING INFORMATION

Additional supporting information can be found online in the Supporting Information section at the end of this article.

How to cite this article: Sartoneva R, Lyyra I, Juusela M, et al. In vitro biocompatibility of polylactide and polybutylene succinate blends for urethral tissue engineering. *J Biomed Mater Res*. 2023;1-13. doi:10.1002/jbm.b.35268